Nanobiotechnology of Marine Organisms: Mechanisms and Applications

19

Sougata Ghosh, Pranav Pandya, and Sirikanjana Thongmee

Abstract

One of the most emerging fields of research in recent decades is nanobiotechnology, which has wide applications in therapeutics, agriculture, and environment. The nanomaterials can be synthesized using physical, chemical, or biological approaches. Unlike physical and chemical methods, biological synthesis of nanoparticles does not need any hazardous conditions or chemicals for reduction of metal ions to their corresponding nanoparticles and their further stabilization. Various bacteria, fungi, algae, plants, and their metabolites are reported for synthesis of metal and metal oxide nanoparticles. Although there is a great diversity in the marine microflora, relatively less research has been carried out with respect to the exploration of their nanobiotechnological potential. This chapter gives an elaborate account on the marine-microbe-mediated synthesis of nanoparticles and their applications. Marine bacteria such as *Enterococcus* sp., *Marinobacter pelagius, Paracoccus haeundaensis, Streptomyces rochei*, and *Vibrio alginolyticus* can synthesize cadmium sulfide (CdSNPs), gold (AuNPs) and silver (AgNPs) nanoparticles. Similarly, halophilic cyanobacteria such as *Phormidium formosum* and *Phormidium tenue* isolated from sea water can synthesize AgNPs and CdSNPs, respectively. Various marine fungi like *Aspergillus sydowii, Cladosporium cladosporioides, Cladosporium halotolerans,* and yeasts such as *Candida* sp. and *Rhodosporidium diobovatum* can synthesize AuNPs and AgNPs

S. Ghosh (✉)
Department of Microbiology, School of Science, RK University, Rajkot, Gujarat, India

Department of Physics, Faculty of Science, Kasetsart University, Bangkok, Thailand

P. Pandya
Department of Microbiology, School of Science, RK University, Rajkot, Gujarat, India

S. Thongmee
Department of Physics, Faculty of Science, Kasetsart University, Bangkok, Thailand

R. Soni et al. (eds.), *Current Status of Marine Water Microbiology*,
https://doi.org/10.1007/978-981-99-5022-5_19

with antimicrobial, antioxidant, and anticancer activities. Likewise, numerous marine algae such as *Amphiroa rigida*, *Caulerpa racemosa, Cystoseria baccata*, *Padina* sp., *Portieria hornemannii*, *Sargassum muticum, Sargassum tenerrimum*, *Spyridia filamentosa*, and *Turbinaria conoides* can synthesize a wide range of stable nanoparticles with promising therapeutic applications. The marine-microbe-synthesized nanoparticles are not only stable but also very small with more surface area and high medicinal properties. Hence, it would be interesting to explore these nanoparticles for development of potent nanomedicine by drug functionalization in order to aim targeted delivery and sustained release.

Keywords
Marine microbes · Nanoparticles · Biogenic synthesis · Bacteria · Fungi · Algae

19.1 Introduction

Marine microorganisms living in the hypersaline environment include several halotolerant bacteria, cyanobacteria, fungi, yeast, and algae. These microbes are widely used for production of various bioactive metabolites that are used in cosmetics, pharmaceutics, food, and agriculture (Zhang et al. 2005; Zhang and Kim 2010). Several anticancer compounds like fucoidans, fucoxanthin, dehydrothyrsiferol, didemnin B, ecteinascidin 743, aplidine, and others are reported from the marine microbes (Shah and Ghosh 2020). Likewise, numerous antimicrobial compounds such as loloatins A–D, myticin, and psammaplin A are reported from marine ascidians, algae, bacteria, bryozoans, sponges, and soft corals. It is important to note that the marine microbes have surface-active functional groups that make them efficient biosorbents. *Marinomonas communis, Marinobacter santoriniensis, Pseudomonas aeruginosa, Enterobacter cloacae, Alteromonas haloplanktis,* and *Vibrio harveyi* of marine origin are well known for removal of toxic metals such as lead, copper, cobalt, cadmium, chromium, and arsenic (Ghosh et al. 2022).

The extracellular polymeric substances (EPSs) produced by marine bacteria is a complex mixture of polysaccharides, glycoproteins, humic-like substances, lipids, uronic acid, and nucleic acids. Likewise, complex capsular polysaccharides (CPSs) or slime polysaccharides are composed of neutral carbohydrates such as arabinose, fructose, galactose, glucose, rhamnose, ribose, and xylose apart from galacturonic and glucuronic acids. Both of these EPS and CPSs play a major role in the adsorption of metal ions (Ruangsomboon et al. 2007). Many marine bacteria can produce siderophores such as aerobactin, anguibactin, alterobactin, aquachelin, biscaberin, vulnibactin, and marinobactin for chelating metals followed by their uptake (Gaonkar and Borkar 2017). Certain marine manganese-oxidizing bacteria (MOB) such as *Bacillus* sp., *Marinobacter* sp., and *Roseobacter* sp., and members from *Algoriphagus, Brevundimonas, Idiomarina,* and *Nitratireductor* genus exhibit high metal bioremoval efficiencies (Zhou et al. 2016). Mercury-resistant bacteria (MRB) with functional *mer* operon can reduce mercury to a water-soluble form, facilitating its biosorption, uptake, bioaccumulation, precipitation, and even efflux (Dash and

Das 2012). Marine *Pseudomonas aeruginosa* and *Pseudomonas putida* express *bmtA* gene-encoded metallothionein protein that can bind to multiple Zn^{2+} ions with enhanced affinity, promoting its bioaccumulation (Naik et al. 2012).

In view of the background, it is interesting to explore the nanobiotechnological potential of the marine microflora. More recently, marine microorganisms are considered as promising cell factories for fabrication of novel metal and metal oxide nanoparticles with exotic shape, size, physico-chemical and opto-electronic properties (Manivasagan et al. 2016). Marine microbe-mediated nanoparticle synthesis is an environmentally benign, rapid, and efficient method (Golinska et al. 2014). This chapter gives a detailed account on recent reports of nanobiotechnological prospects of marine bacteria, cyanobacteria, fungi, yeast, and algae as listed in Table 19.1. Further, the mechanisms of intracellular and/or extracellular syntheses are discussed along with the biomolecules serving as reducing, capping, and stabilizing agents during the nanoparticle synthesis.

19.2 Bacteria

Marine bacteria have developed mechanisms to synthesize nanostructures either intracellularly or extracellularly. Rajeshkumar et al. (2014) isolated *Enterococcus* sp. RMAA from marine water. Initially, the bacteria was cultured in the sterile nutrient broth for 24 h at 37 °C followed by recovery of the cell-free supernatant by centrifugation at 7000 rpm. The cadmium sulfide nanoparticle (CdSNPs) were synthesized by reaction of the supernatant with 1 mM $CdSO_4$ for 24 h at 37 °C for 24 h. UV-visible spectroscopy indicated an intense peak at 410 nm confirming the synthesis of the CdSNPs that were mostly spherical with size ranging from 50 nm to 180 nm as revealed by the scanning electron microscope (SEM) analysis. The strong peaks at 3272 cm^{-1} and 1630 cm^{-1} in Fourier transform infrared (FTIR) spectrum were specific to primary and secondary amines or amide linkages in the protein that might play a significant role in the synthesis and stabilization of the CdSNPs. Promising antimicrobial activity against both bacteria and fungus was exhibited by the CdSNPs. The zones of inhibition (ZOIs) against *Serratia nematodiphila, Escherichia coli, Klebsiella planticola*, *Vibrio* sp., and *Planomicrobium* sp. were 14.16 ± 0.088 mm, 16.16 ± 0.334 mm, 23.27–0.120 mm, 14.30 ± 0.153 mm, and 18.27 ± 0.146 mm, respectively, when treated with 200 μL of the CdSNPs. Similarly, the CdSNPs also showed potent fungicidal activity against *Aspergillus niger* and *Aspergillus flavus*.

Nandhini et al. (2021) derived gold nanoparticles (AuNPs) from marine *Enterococcus* sp. RMAA and analyzed the cytotoxicity of NPs on hepatocellular carcinoma cells (HCCs). The organism was inoculated in nutrient broth and incubated for 24 h in a shaking condition. About 1 mM of gold chloride was added to the broth after 18 h. The UV-Vis spectrum identified the absorbance peak in between 540 and 560 nm for the AuNPs. The TEM analysis revealed the spherical shape of particles. The average size of NPs was 7 nm. The IC_{50} (concentration at which 50% cells are killed) of AuNPs in HepG2 cells was found to be around 10 μg/mL. The

Table 19.1 Nanoparticles synthesized by marine microbes

Source	Nanoparticle	Size (nm)	Shape	Activity/ application	Reference
Bacteria					
Enterococcus sp. RMAA	CdSNPs	50–180	Spherical	Antibacterial and antifungal	Rajeshkumar et al. (2014)
Enterococcus sp. RMAA	AuNPs	7	Spherical	Anticancer	Nandhini et al. (2021)
Marinobacter pelagius RS 11	AuNPs	<20	Spherical, triangular	–	Sharma et al. (2012)
Paracoccus haeundaensis BC74171	AuNPs	20.93 ± 3.46	Spherical	Antioxidant and anticancer	Patil et al. (2019)
Stenotrophomonas	AgNPs,	40–60	Circular, triangular, pentagonal, hexagonal, irregular	–	Malhotra et al. (2013)
Stenotrophomonas	AuNPs	10–50	Spherical, irregular	–	Malhotra et al. (2013)
Streptomyces rochei MHM13	AgNPs	22 to 85	Spherical	Antibacterial and anticancer	Abd-Elnaby et al. (2016)
Vibrio alginolyticus	AuNPs	50–100	Irregular	Anticancer and antioxidant	Shunmugam et al. (2021)
Cyanobacteria					
Phormidium formosum	AgNPs	1–26	Spherical	Antibacterial	Elkomy (2020)
Phormidium tenue NTDM05	CdSNPs	5	Spherical	–	Mubarak Ali et al. (2012)
Fungi and yeast					
Aspergillus sydowii	AuNPs	8.7–15.6	Spherical	–	Vala (2015)
Cladosporium cladosporioides	AgNPs	30–60	Spherical	Antioxidant and antimicrobial	Hulikere and Joshi (2019)
Cladosporium halotolerans	AgNPs	20	Spherical	Antioxidant, antifungal, and anticancer	Ameen et al. (2021)
Candida sp. VITDKGB	AgNPs	87	Spherical and rod shaped	Antibacterial	Dinesh et al. (2011)
Rhodosporidium diobovatum	PbSNPs	2–6	Spherical	–	Seshadri et al. (2011)

(continued)

Table 19.1 (continued)

Source	Nanoparticle	Size (nm)	Shape	Activity/ application	Reference
Algae					
Amphiroa rigida	AgNPs	20–30	Spherical	Antibacterial, anticancer, larvicidal	Gopu et al. (2021)
Caulerpa racemosa	AgNPs	10	Spherical	Antibacterial	Kathiraven et al. (2015)
Caulerpa serrulata	AgNPs	10 ± 2	Spherical	Antibacterial	Aboelfetoh et al. (2017)
Cystoseria baccata	AuNPs	8.4 ± 2.2	Spherical	Anticancer	González-Ballesteros et al. (2017)
Padina sp.	AgNPs	40–45	Spherical, oval, and irregular	Antibacterial	Bhuyar et al. (2020)
Portieria hornemannii	AgNPs	60–70	Spherical	Antibacterial	Fatima et al. (2020)
Sargassum muticum	AuNPs	5.42 ± 1.8	Spherical	–	Namvar et al. (2015)
Sargassum tenerrimum and *Turbinaria conoides*	AuNPs	27.5 and 35	–	Catalytic activity	Ramakrishna et al. (2016)
Spyridia filamentosa	AgNPs	20–30	Spherical	Antibacterial and anticancer	Valarmathi et al. (2020)

AuNP-treated cells showed internal accumulation of reactive oxygen species (ROS) that inhibited the proliferation of HepG2 cells through intracellular ROS-mediated apoptosis and by reducing the concentration of proliferating cell nuclear antigen (PCNA).

Sharma et al. (2012) isolated a novel strain (RS 11) of *Marinobacter pelagius* from solar-salterns that were used for synthesis of gold nanoparticles (AuNPs). The bacteria were grown in Zobell marine broth at 37 °C till they reach the stationary phase. The bacterial biomass was recovered by centrifuging at 12,500 rpm for 15 min at 4 °C followed by washing. The washed cells were resuspended in 10 mL $HAuCl_4$ solution (250 mg/L), and the pH was adjusted to 5–6. Appearance of pink color and an intense peak at 540 nm in UV-visible spectra specific to the surface plasmon resonance confirmed the synthesis of the AuNPs. Mostly spherical and triangular AuNPs were observed, which were less than 20 nm in size as seen in Fig. 19.1. Primary and secondary amines as indicated by the prominent bands at 3027 cm^{-1} and 2977 cm^{-1} were revealed by the FTIR. Further, the bands at 1650 cm^{-1} and 1541 cm^{-1} were also observed that were attributed to the carbonyl stretch and the N-H bonds vibration, respectively, that are associated with the amide I and amide II linkages.

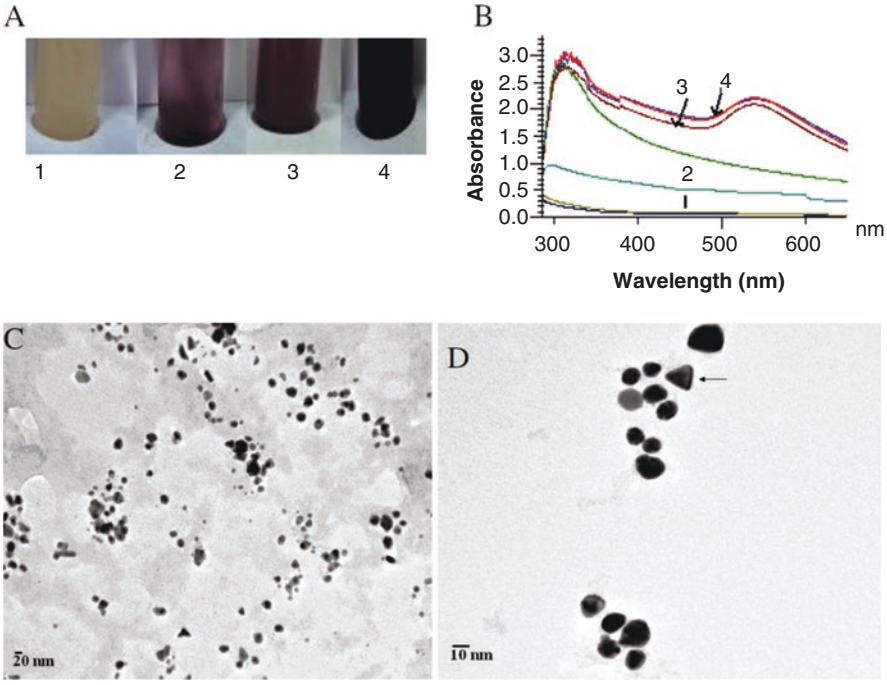

Fig. 19.1 (**a**) Pictures of test tubes containing the bacteria *M. pelagius* cells before (test tube 1) and during incubation in an aqueous of $HAuCl_4$ solution at pH 7.8; (**b**) UV–Vis absorption spectra of gold nanoparticles after the incubation of *M. pelagius* in 1×10^{-3} M aqueous $HAuCl_4$ solution at 7.8 pH. The numbers (Zhang et al. 2005; Zhang and Kim 2010; Shah and Ghosh 2020; Ghosh et al. 2022) indicate the absorption spectra taken at different time intervals 24,48,72, and 96 h, respectively; (**c**, **d**) TEM images of gold nanoparticles produced by the reaction of 1×10^{-3} M aqueous $HAuCl_4$ solution with bacteria *M. pelagius* biomass at 7.8 pH. Particles are mostly spherical with nanotriangles also present (arrow). Bar = 20 nm (**a**) and 10 nm (**b**). (Reprinted from Sharma N, Pinnaka AK, Raje M, Fnu A, Bhattacharyya MS, Choudhury AR (2012) Exploitation of marine bacteria for production of gold nanoparticles. Microb Cell Factories 11:86. https://doi.org/10.1186/1475-2859-11-86 (Open access))

Patil et al. (2019) reported the synthesis of AuNPs by using marine *Paracoccus haeundaensis* BC74171 strain of marine bacteria and also investigated their antioxidant and anticancer properties. A reaction mixture containing 10 mL chloroauric acid (2 mM) and 10 mL of the cell-free supernatant obtained after centrifuging bacteria at 3500 rpm for 30 min at 4 °C was shaken at 70 °C for 15 min in the water bath for synthesis of AuNPs. The pure AuNPs powder was obtained after separation by centrifuging at 13,000 rpm for 25 min followed by washing and lyophilization. The formation of AuNPs was indicated by the appearance of ruby-red color. The UV-Visible spectroscopy indicated the highest absorbance with a sharp peak at 537 nm. The spherical shape, polydispersed nature, and average size of 20.93 ± 3.46 nm were confirmed by TEM analysis. The zeta potential of the NPs was - 4.26 mV. The presence of elemental gold was confirmed by the signal peak at

2.15 keV using EDX (energy dispersion X-ray) analysis. The FTIR (Fourier transformed infrared spectroscopy) analysis of the NPs showed different vibrational bands at 3394, 1639, 1547, 1338, 1408, and 1157 cm^{-1} corresponding to N-H stretching, N-H bending, nitro compounds stretching, C-C aromatic stretching, and C-O stretching, respectively. The proteins and enzymes present in the surrounding reaction mixture were reported to act as reducing and capping agents during AuNPs synthesis. The antioxidant activity of AuNPs tested using 2,2-diphenylpicrylhydrazyl (DPPH) assay revealed the highest radical-scavenging activity of 73.04 ± 3.01% at 320 μg/mL concentration of AuNPs. The anticancer activity of the particles was analyzed against human cell lines such as HEK293 and HaCaT, which were normal cells and AGS and A549 that were cancer cells. The cell viability of AGS cells was 76.46 ± 2.53%, while no effect was observed on the proliferation of normal cells when treated with 200 μg/mL of AuNPs. The mechanism of inhibiting cancer cell proliferation by AuNPs was mainly the alteration of cell growth proteins, DNA fragmentation, and apoptosis.

Malhotra et al. (2013) reported synthesis of AuNPs and AgNPs from *Stenotrophomonas* isolated coral sample, *Pocillopora damicornis* collected from the Mandapam coast, Bay of Bengal, India. Synthesis of AgNPs by the cell-free supernatant was indicated by appearance of intense brick red color, while AuNPs synthesis was confirmed by development of violet color. After 4 h of synthesis, UV-visible observation showed a strong peak at 440 nm that was specific for AgNPs, while the peak for AuNPs was centered at 580 nm. The bacteriogenic AgNPs were circular, triangular, pentagonal, hexagonal, and even irregular in shape, which were in a range 40 to 60 nm. However, the AuNPs were more spherical and irregular shaped with an average particle size ranging between 10 and 50 nm.

Abd-Elnaby et al. (2016) evaluated the antibacterial and anticancer activities of AgNPs synthesized using marine *Streptomyces rochei* MHM13. About 50 mL of 1 mM $AgNO_3$ was mixed with bacterial extract (50 mL) at pH 8.5. The reaction mixture was incubated in darkness at 37 °C under shaking condition (200 rpm) for 5 days. The change in color to yellow-brown gave the visible confirmation of the successful synthesis of the AgNPs. The UV-Vis spectroscopy identified the maximum surface plasmon resonance (SPR) peak at 410 nm for the synthesized AgNPs. The intense absorbance peak of N-H stretching of the amine group was obtained at 3420.14 cm^{-1}, which was revealed from the FTIR spectrum. The amide groups of protein served as a stabilizing or capping agent for the NPs. The spherical shape and size range of 22 to 85 nm of the particles was showed by SEM analysis. The antibacterial activity of AgNPs varied in terms of zone of inhibition against different pathogenic bacteria such as *B. subtilis* (18 mm), *S. aureus* (18 mm), *P. aeruginosa* (18 mm), *Bacillus cereus* (16 mm), *Salmonella typhimurium* (18 mm), *E. coli* (16 mm), *Vibrio fluvialis* (19 mm), and *Vibrio damsela* (16 mm). The antifouling activity (inhibition of bacterial cell density) of AgNPs revealed 99.9% inhibition of *E. coli*. The significant anticancer activity of AgNPs was observed against different cancer cell lines like Hep-G2, HCT-116, A-549, and MCF-7. The highest reduction in viable cells of Hep-G2 (21.63%), MCF-7 (36.42%), HCT-116 (17.97%), PC-3

(48.13%), A-549 (38.59%), CACO (54.31%), HEP-2 (63.82%), and HELA (56.79%) was observed at 50 µg of AgNPs.

Shunmugam et al. (2021) investigated the use of the marine bacteria *Vibrio alginolyticus* for the synthesis of AuNPs and further studied its anticancer and antioxidant activities. The bacterial strain was inoculated, incubated, and centrifuged at 8000 rpm for 15 min to collect the supernatant. The precursor chloroauric acid (HAuCl) was added to the cell free supernatant and the mixture was incubated under shaking conditions for 24 h at 40 °C with 120 rpm. After that the sample was lyophilized and the powder was stored. The initial indication of successful synthesis of AuNPs was the change in color of the final solution from light to dark yellow to reddish brown. The confirmation of AuNPs synthesis by the organism was indicated by the absorbance band obtained at 530 nm when analyzed by UV-Vis spectroscopy. The morphological analysis of AuNPs carried out by SEM revealed the irregular shape of the particles. An average size of 50–100 nm of the AuNPs was identified using TEM. The FTIR results of the particles identified the peaks specific to different functional groups at 1644, 1399, 3542, 2926, and 557 cm^{-1} depicting vibrational stretches of alkene, CH_3, C-H, C-F, and C-Br, respectively. The antioxidant activity of AuNPs analyzed using the DPPH assay showed the maximum radical-scavenging activity at 10 µg/mL concentration of NPs. The AuNPs used for metal-ion-chelating assay showed enhancement by 22.06% in ferrous-ion-chelating activity compared to the untreated samples. The IC_{50} value of 15 µg/mL was obtained for AuNPs while testing the anticancer activity of the particles against colon cancer cell lines (HCA-7). The AuNPs also showed prominent fluorescence in the nucleus.

19.3 Cyanobacteria

Various cyanobacteria are rich in proteins, amino acids, carbohydrates, and sugars, which can be exploited for biosynthesis of diverse nanoparticles (Nitnavare et al. 2022). However, only few reports exist on the nanobiotechnological potential of marine cyanobacteria. In one such report, Elkomy (2020) synthesized AgNPs from a marine cyanobacterium *Phormidium formosum* isolated from the Mediterranean coast of Egypt. Initially, 5 g *P. formosum* biomass was collected from an exponential phase culture growing in F/2 medium, which was then thoroughly washed and reacted with 100 mL of 1 mM aqueous $AgNO_3$ solution for 24 h at pH 7. After completion of the AgNPs synthesis at 28 °C, the reaction mixture was centrifuged at 1200 rpm for 30 min and the pellet was collected followed by drying at 45 °C. Appearance of brown color and absorbance at 437 in UV-visible spectra confirmed the synthesis of AgNPs that were spherical in shape and 1–26 nm in size. FTIR analysis revealed a strong broad band at 3223.11 cm^{-1} that is specific to O-H stretch carboxylic group. The biogenic AgNPs exhibited antimicrobial activity against both *Vibrio* spp. and *Staphylococcus aureus*, with a ZOI equivalent to 27 mm and 22 mm, respectively.

In another interesting study, CdSNPs were synthesized using C-phycoerythrin (C-PE) which is a pigment extracted from the marine cyanobacterium, *Phormidium*

tenue NTDM05 (Mubarak Ali et al. 2012). C-phycoerythrin extract was reacted with 0.25 mM $CdCl_2$ and 1 mM Na_2S aqueous solutions for 5 days. Appearance of orange color and UV-visible absorption peak centred at 470 nm confirmed the synthesis of CdSNPs which were spherical in shape, 5 nm in size and stable up to 8 months. FTIR spectra strongly rationalized the involvement of the thiol group in capping the biogenic CdSNPs.

19.4 Fungi and Yeast

Mycogenic synthesis of nanoparticles is considered most promising due to the rapid, efficient, and stable nature. Vala (2015) reported AuNPs from marine fungus, *Aspergillus sydowii*, isolated from Gulf of Khambhat, West Coast of India. Fungal biomass was generated by inoculating 1 mL of spore suspension (~ 10^6/mL) in potato dextrose medium prepared in 75% "aged" seawater. After 4 days of incubation, the biomass was recovered by filtration, which was then washed in distilled water. Various concentrations of gold chloride (0.25 to 3 mM) were reacted with 5 g of fungal biomass under static condition for 72 h at 27 °C. Development of purple-lavender color within 18 h or reaction with 0.25 and 0.5 mM gold chloride indicated formation of larger AuNPs. On the other hand, pink color was obtained with 2 and 3 mM gold salt concentration, suggesting formation of AuNPs of small size. It was speculated that the fungal enzymes might be responsible for the reduction of Au^{3+} to Au^0, while the proteins might have capped the mycogenic AuNPs, making them more stable. Monodispersed spherical AuNPs were in a size range of 8.7–15.6 nm with a mean diameter of 10 nm.

Hulikere and Joshi (2019) employed marine endophytic fungus, *Cladosporium cladosporioides*, for the AgNPs synthesis and also tested its antioxidant and antimicrobial activities. The mycelial biomass was cultivated, filtered, and washed with distilled water. The biomass was further incubated for 48 h at room temperature and the final synthesis of AgNPs was carried out after mixing 10 mL of filtrate and 90 mL of 1 mM $AgNO_3$. Appearance of dark brown confirmed the formation of AgNPs. The strong peak for the AgNPs at 440 nm was noted by UV-Vis spectroscopy. The field emission SEM (FESEM) revealed the uniformly spherical shape of the particle. The size of the particles were in a range from 30 to 60 nm. The crystalline nature of the particle was identified by XRD analysis. The FTIR analysis identified O-H stretching vibrations of alcohol and phenolic groups (3338 cm^{-1}), O-H stretching of carboxylic acids (2331 cm^{-1}), C-O amide stretching (1640 cm^{-1}), and C-N amine stretching (1323 cm^{-1}). Capping and reduction were attributed to the fungal proteins, enzymes, and polyphenols present in the extract. The biosynthesis of AgNPs was achieved by the combination of electron shuttles and NADPH-dependent reductases. The mycogenic AgNPs showed promising antimicrobial activity with a ZOI of 7.5 ± 2.0 mm, 9.2 ± 0.4 mm, 10.5 ± 2.5 mm, 8.4 ± 0.1 mm, 7.2 ± 3.5 mm against *S. aureus, S. epidermis, B. substilis, E. coli,* and *C. albicans*, respectively. ROS associated cell membrane disruption and damage to DNA and proteins were speculated as prominent mechanisms for the antimicrobial activity.

Ameen et al. (2021) reported the synthesis of AgNPs from the marine fungus *Cladosporium halotolerans* and investigated its antioxidant, antifungal and anticancer properties. About 90 mL of biomass filtrate and 10 mL of $AgNO_3$ (1 mM) were mixed and incubated in a shaker for 30 min. The color change from pure white to black represented the visual confirmation of AgNPs formation. The peak obtained at 500 nm using UV-Vis spectroscopy confirmed the formation of AgNPs. The XRD analysis identified the crystalline structure of the particle. From the classical Scherrer formula the size of particle was evaluated as 20 nm. The FTIR analysis revealed the peaks defining different functional groups like -OH group (1078 and 3315 cm^{-1}) and alkenes (1644 cm^{-1}) that might have taken part in the synthesis and stabilization of the AgNPs. SEM showed uniformly spherical AgNPs with 64.2% silver as analyzed using EDX. The zeta potential of the particles was −51.8 mV. TEM analysis showed that the spherical AgNPs with smooth surface were 20 nm in size as evident from Fig. 19.2. DPPH radical-scavenging activity of the mycogenic AgNPs was dose dependent where 78% antioxidant activity was noted within 30 min of incubation. The IC_{50} value for anticancer activity of AgNPs was 34.27 µL/mL against MCF-7 cells. The antifungal activity of AgNPs against *A. niger* showed dose-dependent response that was equivalent to 45% and 70% inhibition at 500 ppm and 1000 ppm of AgNPs, respectively.

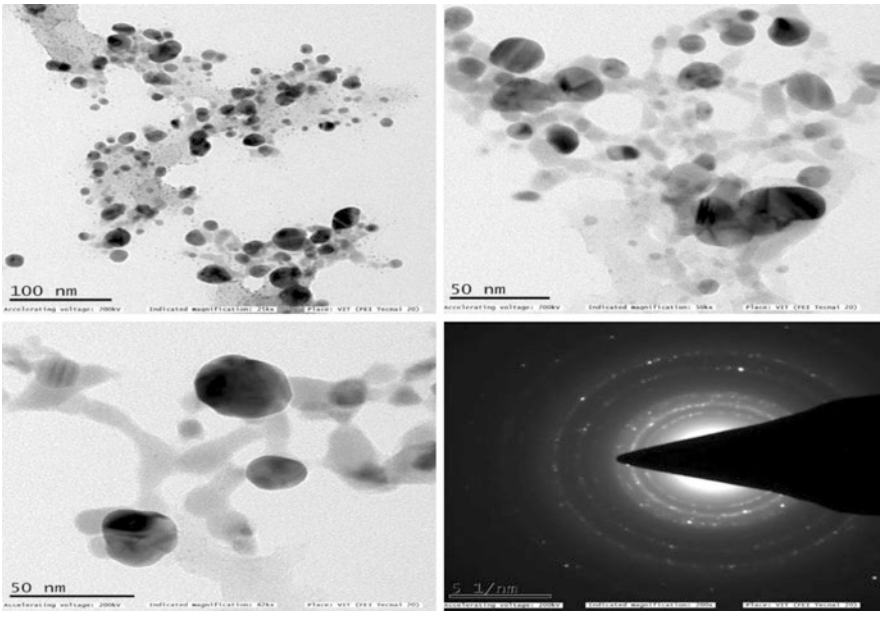

Fig. 19.2 TEM images of AgNPs synthesized using *C. halotolerans.* (Reprinted with permission from Ameen F, Al-Homaidan AA, Al-Sabri A, Almansob A, AlNAdhari S (2021) Anti-oxidant, anti-fungal and cytotoxic effects of silver nanoparticles synthesized using marine fungus *Cladosporium halotolerans*. Appl Nanosci 1–9. https://doi.org/10.1007/s13204-021-01874-9. Copyright © 2021, King Abdulaziz City for Science and Technology)

Novel marine yeast, *Candida* sp. VITDKGB, isolated from the coastal areas of Nicobar Islands, India, was used for synthesis of AgNPs with promising antimicrobial activity against multidrug-resistant (MDR) pathogens (Dinesh et al. 2011). The silver-tolerant strain of the yeast was inoculated in 100 mL sterile Sabauroud's dextrose broth prepared in 50% marine water and incubated 48 h at 35 °C under shaking condition (120 rpm). The biomass was then recovered by centrifuging the broth 10,000 rpm for 10 min at 4 °C. The supernatant was collected and reacted with 1 mM $AgNO_3$ for 48 h at 35 °C in darkness under shaking condition (120 rpm). UV-visible spectra showed an intense peak at 430 nm attributed to the SPR of AgNPs, which was mostly spherical and rod shaped. The particles were 87 nm in size as evaluated from atomic force microscope (AFM) measurements. FTIR analysis revealed the bands at 3442.97 cm^{-1}, 1383.16 cm^{-1}, 2927.34 cm^{-1}, 1631.31 cm^{-1}, 1224.76 cm^{-1}, 1062.49 cm^{-1}, and 643.72 cm^{-1} which are associated with stretching vibration of primary amines, C-N stretching of amines, aliphatic—CH_3 and CH_2 stretching, -NHCO of amide, ester carbonyl group/phenol, C-O stretching of polysaccharides/Si-O asymmetric stretch and CH out of plane bending of carbohydrate, respectively. The AgNPs exhibited antibacterial activity with ZOI equivalent to 7.33 ± 0.57 and 5.66 ± 0.57 mm against MDR *S. aureus* and *K. pneumoniae*, respectively.

Seshadri et al. (2011) reported synthesis of lead sulfide nanoparticles (PbSNPs) using *Rhodosporidium diobovatum*, a marine yeast isolated from Indian Ocean. The cells in the log phase accumulated 55% lead intracellularly when grown in lead-nitrate-supplemented culture medium. Also 26% and 90.52% lead accumulation was noted in the beginning and the end of the stationary phase (96 h), respectively. The resulting PbSNPs were spherical and well dispersed showing a large blue shift in the absorption edge to ~320 nm. The size of the nanoparticles was in a range from 2 to 6 nm. Phytochelatins were reported to cap the PbSNPs, resulting in their stability. Such thiol compounds not only detoxify the nanoparticle but also prevent agglomeration of the same.

19.5 Algae

Algae are aquatic photosynthetic microbes that are widely used for synthesis of various nanoparticles. Gopu et al. (2021) utilized marine red algae *Amphiroa rigida* (AR) collected from coastal area of Kanyakumari District, Tamil Nadu, India, for the synthesis of AgNPs. Initially, the algal biomass was shade-dried and pulverized into fine powder in order to increase the surface area. Then 10 g of the algal powder was suspended in 500 mL of double-distilled water and extracted for 20 min at 80 °C for 20 min under stirring condition. The extract was filtered and centrifuged at 10,000 rpm for 10 min. A 10 mL of AR supernatant was mixed with 90 mL $AgNO_3$ (1 mM) solution. The mixture was incubated at 37 °C till reddish brown color appeared. After the completion of the reaction, the AgNPs were centrifuged at 9000 rpm for 15 min (4 °C). The particles were washed and repeatedly centrifuged using double-distilled water for complete removal of the impurities. The successful

formation of AgNPs was confirmed by the absorption band obtained at 420 nm as indicated in the UV-Vis spectroscopy. The average size of the particle from Debye-Scherer's equation was around 25 nm. The TEM analysis showed spherical particles with an average size of 20–30 nm. The FTIR spectroscopy showed the prominent peaks for OH stretching and CH stretching vibrations of hydroxyl groups (2382.87 cm^{-1}), C=O stretching (1701.22 and 1512.19 cm^{-1}), and C-O stretching in ether groups (1147.65 cm^{-1}). The bioactive compounds such as phenolic, ether, and polysaccharides were involved in the bio-reduction of Ag^{+} to Ag^{0}. The resulting AgNPs exhibited antibacterial effect against *S. aureus* and *P. aeruginosa* with ZOI equivalent to 21 ± 0.2 mm and 15 ± 0.2 mm, respectively as seen in Fig. 19.3. The minimum inhibitory concentration (MIC) values were evaluated as 3.125 and 6.25 μg/mL, respectively. The AgNPs inhibited breast cancer cell lines (MCF-7) with an IC_{50} value of 20 μg/mL. The highest mortality (100%) against third instar larva of *Aedes aegypti* was achieved on treatment with 20 μg of AgNPs, while for the fourth instar larva, the highest mortality was caused by 40 μg of AgNPs.

Kathiraven et al. (2015) demonstrated the synthesis of AgNPs using marine algae *Caulerpa racemosa* collected from the Gulf of Mannar, Southeast coast of India. The synthesis of AgNPs was carried out by reacting 10 mL of algal filtrate with 90 mL of $AgNO_3$ (10^{-3} M) at room temperature. The synthesis of AgNPs was accompanied by initial appearance of light-yellow color that gradually intensified to

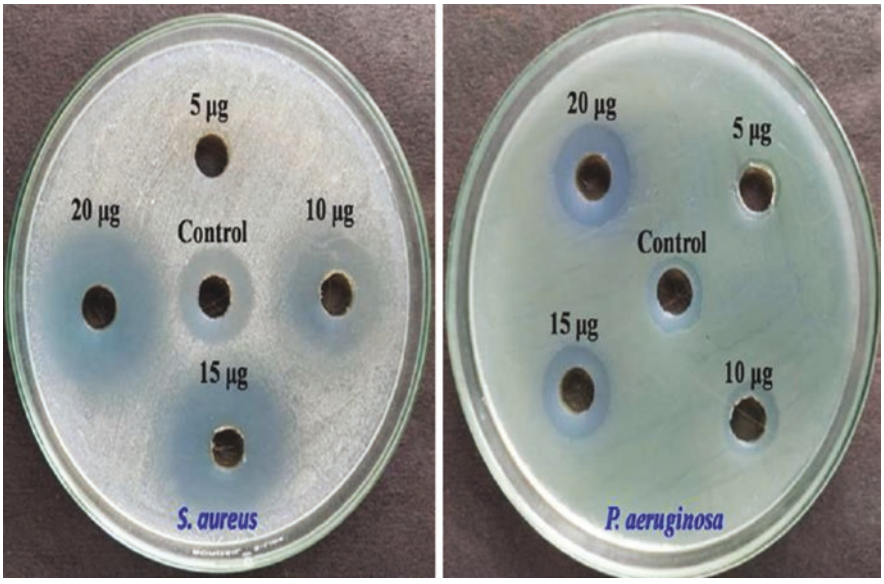

Fig. 19.3 Antibacterial effect of AR-AgNPs against human pathogens. (Reprinted with permission from Gopu M, Kumar P, Selvankumar T, Senthilkumar B, Sudhakar C, Govarthanan M, Selvam K (2021) Green biomimetic silver nanoparticles utilizing the red algae *Amphiroa rigida* and its potent antibacterial, cytotoxicity and larvicidal efficiency. Bioprocess Biosyst Eng 44 (2):217–223. https://doi.org/10.1007/s00449-020-02426-1 Copyright © Springer-Verlag GmbH Germany, part of Springer Nature 2020)

brown color. UV-Vis spectra showed a maximum absorbance peak at 413 nm that is specific to the SPR of AgNPs. The FTIR spectrum for the synthesized AgNPs identified the peaks of OH-stretching vibrations (3440 cm^{-1}) and (NH) = O group stretching (1639 cm^{-1}). The shifting in band from 1631 to 1639 cm^{-1} was reported due to the binding of (NH)C=O group with the particles. The TEM images revealed the spherical shape of the particles, which were 10 nm in size. The antibacterial efficiency of the particles studied through well diffusion assay against *Proteus mirabilis* and *S. aureus* showed the ZOI of 14 mm and 7 mm, respectively.

In another study, Aboelfetoh et al. (2017) fabricated AgNPs by using *Caulerpa serrulata* (green marine algae) that was collected from Red Sea coast, Egypt. The particles were synthesized by adding 5–25 mL of algal extract to 10^{-3} M $AgNO_3$ solution. The change in color of the solution from yellow to reddish brown indicated the formation of AgNPs. The UV-Vis spectral analysis also confirmed the color change of the solution. On increasing the extract concentration from 5% to 25%, the intensity of the SPR band was noted that might be attributed to the aggregation of the particles. Lower pH resulted in the formation of more AgNPs with smaller diameter. FTIR analysis indicated different peaks at 3447, 1730, 2929, 2859, 1613, 1194, 1125, 1023, 2300–2336 cm^{-1} that represents O-H, C=O C-H, C=C, C-O, C ≡ C stretching vibrations. The XRD analysis confirmed the crystallinity of the phycogenic AgNPs with a face-centered cubic structure. The spherical morphology of the AgNPs with an average size of 10 ± 2 nm was observed in the HRTEM images. The antibacterial activity of AgNPs against *E. coli* and *Salmonella typhi* was indicated by ZOI equivalent to 21 mm and 10 mm, respectively. The toxicity of AgNPs toward these organisms was mainly attributed to the disruption of the cell wall and increase in the permeability of the plasma membrane.

González-Ballesteros et al. (2017) demonstrated the synthesis of AuNPs by utilizing marine brown algae *Cystoseria baccata* (CB) collected from the lower intertidal rocky shore in the NW coast of Spain. About 75 μL of 0.01 M $HAuCl_4$ was mixed with 1 mL of CB extract and the mixture was stirred at room temperature for 24 h. The change in pH of the CB extract from 5.4 to 4.5 was noted during formation of the AuNPs. The 0.4 mM concentration of AuNPs was considered optimum. The characteristic peak observed at 532 nm is specific to the SPR of AuNPs. The zeta potential of the particle was −30.7 ± 2.0 mV. The TEM images revealed the spherical AuNPs with 8.4 ± 2.2 nm average size. The HRTEM studies identified the polycrystalline nature of the particles, while the elemental mapping confirmed the presence of carbon in the surrounding of AuNPs. The FTIR spectrum identified the peaks at 3402, 2937, 1662, 1417, 1078, and 1254 cm^{-1} attributing to NH or OH stretching, CH stretching, strong asymmetric stretching of carbonyl, weak symmetric stretching of carbonyl, C-OH vibrations of primary alcohol, and -SO_3 stretching, respectively. Treatment with the AuNPs resulted in 48-fold and threefold enhancement in early apoptotic cells in colon cancer cells, Caco-2 and HT-29 cells, respectively. The extrinsic pathway was found to be activated in Caco-2 cells, while both extrinsic and intrinsic apoptotic pathways were activated in the case of HT-29 cells by the AuNPs.

Bhuyar et al. (2020) utilized marine macroalgae *Padina* sp. collected from Mersing, Johor, at Peninsular Malaysia for the synthesis of AgNPs. The aqueous algal extract was prepared by mixing 30 g of algal powder and 300 mL of distilled water in 1:10 ratio. The reaction mixture was heated for 20 min at 60 °C and was further filtered. Reaction between 20 mL of algal extract and 180 mL of $AgNO_3$ (0.01 M) at 60 °C for 48 h under stirring condition resulted in the formation of the AgNPs in dark condition. The color change from yellow-brown to concentrated dark brown indicated the synthesis of the AgNPs. The reaction mixture was harvested after 48 h and centrifuged at 8000 rpm for 30 min at 30 °C followed by recovery of the AgNPs pellet that was further dried at 50 °C for 5 h resulting in a yield of 510 mg. The characteristic absorbance band at 445 nm for the AgNPs in UV-Vis spectra confirmed the successful formation of the AgNPs. The FTIR analysis of the extract revealed peaks of O-H and C=O stretching of hydroxyl and carboxylic acid groups (3350.07, 1637.74, 1106.90 cm^{-1}) and N-H stretching vibrations of peptide linkages and hydroxyl stretch of polyphenols (3350.07 cm^{-1}). Average size of the AgNPs according to the SEM analysis was 33.75 nm. FESEM analysis confirmed that the average size of the AgNPs was 40.45 nm. Polydispersed AgNPs showed spherical, oval, and irregular shapes. EDX spectrum confirmed the presence of 85.02 wt% Ag, 9.04 wt% chloride, and 1.35 wt% carbon in AgNPs. The antibacterial activity of the AgNPs was confirmed from the ZOI of 15.17 ± 0.58 mm, 12.67 ± 0.76 mm, 13.33 ± 0.76 mm, 12.67 ± 0.58 mm against *S. aureus*, *B. subtilis*, *P. aeruginosa*, and *E. coli*, respectively.

In another similar study, Fatima et al. (2020) studied the antibacterial activity of AgNPs synthesized using marine red algae *Portieria hornemannii* collected from Gulf of Mannar, India. The 1 mM $AgNO_3$ (45 mL) was reacted with 5 mL of algal extract and the mixture was stirred continuously at room temperature. Appearance of dark brown color after 48 h indicated the formation of AgNPs that also showed an SPR-associated absorbance peak at 420 nm in the UV-Vis spectra. The FTIR analysis identified the peaks of C-CI stretching, C-N stretching in aliphatic amines, O-C bond (acids), C-O-H bending of carboxylic classes, O-H, C-H, O-H stretching, and N-H groups at 860, 1076 and 1157, 1261, 1380 and 1400, 2862, 2926, 3147, and 3415 cm^{-1}, respectively. SEM analysis showed spherical shape of the AgNPs, which were 70–75 nm in size. The TEM analysis also confirmed the size of the phycogenic AgNPs to be around 60–70 nm. The zeta potential was about −44.5 mV. The antibacterial activity of the AgNPs tested against *Vibrio harveyii*, *Vibrio anguillarum*, *Vibrio parahaemolyticus*, and *Vibrio vulnificus* was confirmed from their MICs, which were 7.81, 3.9, 7.81, and 15.62 μg/mL, respectively.

Namvar et al. (2015) explored the synthesis of AuNPs by using the marine microalgae *Sargassum muticum* collected from the coastal areas of Persian Gulf. The algal powder was mixed with water and heated at 100 °C followed by filtration. The aqueous extract (50 mL) was reacted with identical volume of 0.1 mM $HAuCl_4$ and stirred at 45 °C till light purple color appeared. The AuNPs pellet was collected after centrifuging the solution at 6000 rpm for 10 min. The absorbance peak of the AuNPs in UV-Vis spectra was at 520 nm. The particles were stable in a pH range of

5–9. TEM images showed that the spherical AuNPs were 5.42 ± 1.8 nm in size. The zeta potential was −35.8 mV.

Ramakrishna et al. (2016) evaluated the catalytic activity of the AuNPs synthesized from two marine brown algae *Sargassum tenerrimum* and *Turbinaria conoides*. The 5 mL aqueous extracts of the algae were mixed with 45 mL $HAuCl_4$ (1 mM). The reaction mixture was stirred and the appearance of ruby red color of the solution indicated the formation of AuNPs. The AuNPs were washed by repeated centrifugation for 15 min at 10,000 rpm and redispersion of the pellet. The intense absorbance peak at 540 nm and broader peaks between 700 and 800 nm were observed for AuNPs. FTIR analysis of the synthesized particle revealed the involvement of amine and hydroxyl functional groups in the synthesis and stabilization of AuNPs. The TEM analysis revealed the anisotropic and polydispersed AuNPs with average diameter of 27.5 nm and 35 nm when synthesized by *T. conoides* and *S. tenerrimum* extracts, respectively. The dynamic light scattering (DLS) analysis confirmed the hydrodynamic radius as 28.60 ± 20.65 nm and 82.30 ± 52.82 nm with a polydispersity index (PDI) of 0.521 and 0.412, when synthesized from *T. conoides* and *S. tenerrimum*, respectively. The zeta potential values of AuNPs derived from *T. conoides* and *S. tenerrium* were −26.3 mV and −29.1 mV, respectively. The catalytic activity of AuNPs was tested on 4-nitrophenol, p-nitroaniline, rhodamine B, and sulforhodamine 101. Catalytic conversion of nitroarene (4-nitrophenol) to its corresponding aminoarenes (4-aminophenol) by AuNPs from *T. conoides* was indicated by the decrease in the absorption peak at 400 nm with concomitant appearance of the peak at 298 nm. The reaction was completed in 300 s with a rate constant (k) of 9.37×10^{-3} s^{-1} and 10.64×10^{-3} s^{-1} for AuNPs from *T. conoides* and *S. tenerrimum*, respectively. Catalytic conversion of p-nitroaniline (p-NA) to *p*-phenylenediamine in presence of AuNPs was indicated by the reduction of peak at 380 nm with simultaneous increase in the peak at 238 nm. The catalytic conversion completed within 123 s and 140 s with rate constants (k) of 18.73×10^{-3} s^{-1} and 16.07×10^{-3} s^{-1} for AuNPs from *T. conoides* and *S. tenerrimum*, respectively. A dose-dependent catalytic reduction of rhodamine B and sulforhodamine 101 was observed.

Valarmathi et al. (2020) developed a route for biogenic synthesis of AgNPs from the marine red algae *Spyridia filamentosa* collected from coastal area of Kanyakumari District, Tamil Nadu, India. The reaction mixture containing 20 mL of *S. filamentosa* extract and 80 mL of 1 mM $AgNO_3$ was incubated at 37 °C for 2 h. On synthesis of the AgNPs, brown color developed and a peak at 420 nm appeared in the UV-vis spectra. The phycogenic AgNPs were spherical in shape and were 20–30 nm in size. The FTIR spectrum showed bands at 3402, 2922 and 2852, 1652 and 1456, and 1099 and 617 attributing hydroxyl and carbonyl groups, methyl group, carboxyl group stretching, and carboxylic acids, ether, and alcoholic groups, respectively. AgNPs inhibited the growth of *Klebsiella* sp. and *Staphylococcus* sp. up to 63.4% and 44.6%, respectively. The biogenic AgNPs were cytotoxic against MCF-7 cells and induced apoptosis.

19.6 Conclusion and Future Perspectives

More recently, biogenic route for synthesis of metal and metal oxide nanoparticles has gained wide attention due to their ease of synthesis, biocompatibility, and stability (Ghosh et al. 2016a, b). Cellular metabolites like reducing sugars, ascorbic acid, citric acid, starch, proteins, enzymes, and others play a significant role in reducing the metal ions to their corresponding nanoparticles and their further stabilization (Bloch et al. 2021; Ghosh 2018). Recent studies have identified the marine microflora as untapped "nanofactories" for the production of metallic nanoparticles due to their rich diversity in metabolites. A major drawback in biogenic nanoparticles is the control of the size and shape. Careful optimization of reaction parameters like time, temperature, pH, metal salt concentration, and cell extract concentration can help to get monodispersed nanoparticles with desired physical and chemical properties (Shende et al. 2017, 2018). At present, very limited reports are available on the therapeutic applications of the nanoparticles synthesized by the marine microorganisms. Hence, antimicrobial, antibiofilm, anticancer, antidiabetic, and antioxidant activities should be evaluated thoroughly to develop more biocompatible nanomedicine (Shinde et al. 2018; Bhagwat et al. 2018). Further, these biogenic nanoparticles can be used for functionalization of drugs for targeted delivery and sustained release that would synergistically enhance the therapeutic index of the drugs (Ghosh 2019; Ranpariya et al. 2021). Bimetallic and alloy nanocomposites would be more potent candidate nanocatalysts due to their enhanced dye-degrading properties that can be employed to treat industrial effluents (Bloch et al. 2022; Tawre et al. 2022; Gami et al. 2022).

In conclusion, marine microbes can be used as promising candidates for synthesis of novel metal nanoparticles with multivariate applications in therapeutics, agriculture, environment, and food industries. Integrated approach using metabolomics, proteomics, and genomics, would help to identify the exact mechanism of synthesis of the nanoparticles by the microbial cell factories.

Acknowledgement Dr. Sougata Ghosh acknowledges Kasetsart University, Bangkok, Thailand, for Postdoctoral Fellowship and funding under Reinventing University Program (Ref. No. 6501.0207/9219 dated 14th September, 2022).

References

Abd-Elnaby HM, Abo-Elala GM, Abdel-Raouf UM, Hamed MM (2016) Antibacterial and anticancer activity of extracellular synthesized silver nanoparticles from marine *Streptomyces rochei* MHM13. Egypt J Aquat Res 42(3):301–312. https://doi.org/10.1016/j.ejar.2016.05.004

Aboelfetoh EF, El-Shenody RA, Ghobara MM (2017) Eco-friendly synthesis of silver nanoparticles using green algae (*Caulerpa serrulata*): reaction optimization, catalytic and antibacterial activities. Environ Monit Assess 189(7):1–15. https://doi.org/10.1007/s10661-017-6033-0

Ameen F, Al-Homaidan AA, Al-Sabri A, Almansob A, AlNadhari S (2021) Anti-oxidant, anti-fungal and cytotoxic effects of silver nanoparticles synthesized using marine fungus *Cladosporium halotolerans*. Appl Nanosci:1–9. https://doi.org/10.1007/s13204-021-01874-9

Bhagwat TR, Joshi KA, Parihar VS, Asok A, Bellare J, Ghosh S (2018) Biogenic copper nanoparticles from medicinal plants as novel antidiabetic nanomedicine. World J Pharm Res 7(4):183–196

Bhuyar P, Rahim MHA, Sundararaju S, Ramaraj R, Maniam GP, Govindan N (2020) Synthesis of silver nanoparticles using marine macroalgae *Padina* sp. and its antibacterial activity towards pathogenic bacteria. Beni-Suef Univ J Basic Appl Sci 9(1):1–15. https://doi.org/10.1186/s43088-019-0031-y

Bloch K, Pardesi K, Satriano C, Ghosh S (2021) Bacteriogenic platinum nanoparticles for application in nanomedicine. Front Chem 9:624344. https://doi.org/10.3389/fchem.2021.624344

Bloch K, Mohammed SM, Karmakar S, Shukla S, Asok A, Thongmee S, Ghosh S (2022) Catalytic dye degradation by novel phytofabricated silver doped zinc oxide nanocomposites. Front Chem 10:1013077. https://doi.org/10.3389/fchem.2022.1013077

Dash HR, Das S (2012) Bioremediation of mercury and the importance of bacterial mer genes. Int Biodeter Biodegr 75:207–213. https://doi.org/10.1016/j.ibiod.2012.07.023

Dinesh KS, Karthik L, Gaurav K, Bhaskara RKV (2011) Biosynthesis of silver nanoparticles from marine yeast and their antimicrobial activity against multidrug resistant pathogens. Pharmacology 3:1100–1111

Elkomy RG (2020) Antimicrobial screening of silver nanoparticles synthesized by marine cyanobacterium *Phormidium formosum*. Iran J Microbiol 12(3):242–248. https://doi.org/10.18502/ijm.v12i3.3242

Fatima R, Priya M, Indurthi L, Radhakrishnan V, Sudhakaran R (2020) Biosynthesis of silver nanoparticles using red algae *Portieria hornemannii* and its antibacterial activity against fish pathogens. Microb Pathog 138:103780. https://doi.org/10.1016/j.micpath.2019.103780

Gami B, Bloch K, Mohammed SM, Karmakar S, Shukla S, Asok A, Thongmee S, Ghosh S (2022) *Leucophyllum frutescens* mediated synthesis of silver and gold nanoparticles for catalytic dye degradation. Front Chem 10:932416. https://doi.org/10.3389/fchem.2022.932416

Gaonkar T, Borkar S (2017) Applications of siderophore producing marine bacteria in bioremediation of metals and organic compounds. In: Naik M, Dubey S (eds) Marine Pollution and Microbial Remediation. Springer, Singapore, pp 177–187. https://doi.org/10.1007/978-981-10-1044-6_11

Ghosh S (2018) Copper and palladium nanostructures: a bacteriogenic approach. Appl Microbiol Biotechnol 102(18):7693–7701. https://doi.org/10.1007/s00253-018-9180-5

Ghosh S (2019) Mesoporous silica based nano drug delivery system synthesis, characterization and applications. In: Mohapatra SS, Ranjan S, Dasgupta N, Mishra RK, Thomas S (eds) Nanocarriers for drug delivery. Elsevier, Amsterdam, pp 285–317. ISBN: 978-0-12-814033-8. https://doi.org/10.1016/B978-0-12-814033-8.00009-6

Ghosh S, Chacko MJ, Harke AN, Gurav SP, Joshi KA, Dhepe A, Kulkarni AS, Shinde VS, Parihar VS, Asok A, Banerjee K, Kamble N, Bellare J, Chopade BA (2016a) *Barleria prionitis* leaf mediated synthesis of silver and gold nanocatalysts. J Nanomed Nanotechnol 7(4):394. https://doi.org/10.4172/2157-7439.1000394

Ghosh S, Gurav SP, Harke AN, Chacko MJ, Joshi KA, Dhepe A, Charolkar C, Shinde VS, Kitture R, Parihar VS, Banerjee K, Kamble N, Bellare J, Chopade BA (2016b) *Dioscorea oppositifolia* mediated synthesis of gold and silver nanoparticles with catalytic activity. J Nanomed Nanotechnol 7(5):398. https://doi.org/10.4172/2157-7439.1000398

Ghosh S, Bhattacharya J, Nitnavare R, Webster TJ (2022) Microbial remediation of metals by marine bacteria. In: Shah MP, Couto SR (eds) Development in wastewater treatment research and processes: microbial degradation of xenobiotics through bacterial and fungal approach. Elsevier, New York, pp 131–158. Paperback ISBN: 978-0-323-85839-7; eBook ISBN: 978-0-323-89793-8. https://doi.org/10.1016/B978-0-323-85839-7.00011-6

Golinska P, Wypij M, Ingle AP, Gupta I, Dahm H, Rai M (2014) Biogenic synthesis of metal nanoparticles from actinomycetes: biomedical applications and cytotoxicity. Appl Microbiol Biotechnol 98(19):8083–8097. https://doi.org/10.1007/s00253-014-5953-7

González-Ballesteros N, Prado-López S, Rodríguez-González JB, Lastra M, Rodríguez-Argüelles M (2017) Green synthesis of gold nanoparticles using brown algae *Cystoseira baccata*: its activ-

ity in colon cancer cells. Colloids Surf B Biointerfaces 153:190–198. https://doi.org/10.1016/j.colsurfb.2017.02.020

Gopu M, Kumar P, Selvankumar T, Senthilkumar B, Sudhakar C, Govarthanan M, Selvam K (2021) Green biomimetic silver nanoparticles utilizing the red algae *Amphiroa rigida* and its potent antibacterial, cytotoxicity and larvicidal efficiency. Bioprocess Biosyst Eng 44(2):217–223. https://doi.org/10.1007/s00449-020-02426-1

Hulikere MM, Joshi CG (2019) Characterization, antioxidant and antimicrobial activity of silver nanoparticles synthesized using marine endophytic fungus-*Cladosporium cladosporioides*. Process Biochem 82:199–204. https://doi.org/10.1016/j.procbio.2019.04.011

Kathiraven T, Sundaramanickam A, Shanmugam N, Balasubramanian T (2015) Green synthesis of silver nanoparticles using marine algae *Caulerpa racemosa* and their antibacterial activity against some human pathogens. Appl Nanosci 5(4):499–504. https://doi.org/10.1007/s13204-014-0341-2

Malhotra A, Dolma K, Kaur N, Rathore YS, Mayilraj S, Choudhury AR (2013) Biosynthesis of gold and silver nanoparticles using a novel marine strain of *Stenotrophomonas*. Bioresour Technol 142:727–731. https://doi.org/10.1016/j.biortech.2013.05.109

Manivasagan P, Nam SY, Oh J (2016) Marine microorganisms as potential biofactories for synthesis of metallic nanoparticles. Crit Rev Microbiol 42(6):1007–1019. https://doi.org/10.3109/1040841X.2015.1137860

Mubarak Ali D, Gopinath V, Rameshbabu N, Thajuddin N (2012) Synthesis and characterization of CdS nanoparticles using C-phycoerythrin from the marine cyanobacteria. Mater Lett 74:8–11. https://doi.org/10.1016/j.matlet.2012.01.026

Naik MM, Pandey A, Dubey SK (2012) *Pseudomonas aeruginosa* strain WI-1 from Mandovi estuary possesses metallothionein to alleviate lead toxicity and promotes plant growth. Ecotoxicol Environ Saf 79:129–133. https://doi.org/10.1016/j.ecoenv.2011.12.015

Namvar F, Azizi S, Ahmad MB, Shameli K, Mohamad R, Mahdavi M, Tahir PM (2015) Green synthesis and characterization of gold nanoparticles using the marine macroalgae *Sargassum muticum*. Res Chem Intermed 41(8):5723–5730. https://doi.org/10.1007/s11164-014-1696-4

Nandhini JT, Ezhilarasan D, Rajeshkumar S (2021) An ecofriendly synthesized gold nanoparticles induces cytotoxicity via apoptosis in HepG2 cells. Environ Toxicol 36(1):24–32. https://doi.org/10.1002/tox.23007

Nitnavare R, Bhattacharya J, Thongmee S, Ghosh S (2022) Photosynthetic microbes in nanobiotechnology: applications and perspectives. Sci Total Environ 841:156457. https://doi.org/10.1016/j.scitotenv.2022.156457

Patil MP, Kang MJ, Niyonizigiye I, Singh A, Kim JO, Seo YB, Kim GD (2019) Extracellular synthesis of gold nanoparticles using the marine bacterium *Paracoccus haeundaensis* BC74171T and evaluation of their antioxidant activity and antiproliferative effect on normal and cancer cell lines. Colloids Surf B Biointerfaces 183:110455. https://doi.org/10.1016/j.colsurfb.2019.110455

Rajeshkumar S, Ponnanikajamideen M, Malarkodi C, Malini M, Annadurai G (2014) Microbe-mediated synthesis of antimicrobial semiconductor nanoparticles by marine bacteria. J Nanostruct Chem 4(2):1–7. https://doi.org/10.1007/s40097-014-0096-z

Ramakrishna M, Rajesh Babu D, Gengan RM, Chandra S, Nageswara Rao G (2016) Green synthesis of gold nanoparticles using marine algae and evaluation of their catalytic activity. J Nanostruct Chem 6(1):1–13. https://doi.org/10.1007/s40097-015-0173-y

Ranpariya B, Salunke G, Karmakar S, Babiya K, Sutar S, Kadoo N, Kumbhakar P, Ghosh S (2021) Antimicrobial synergy of silver-platinum nanohybrids with antibiotics. Front Microbiol 11:610968. https://doi.org/10.3389/fmicb.2020.610968

Ruangsomboon S, Chidthaisong A, Bunnag B, Inthorn D, Harvey NW (2007) Lead (Pb^{2+}) adsorption characteristics and sugar composition of capsular polysaccharides of cyanobacterium *Calothrix marchica*. Songklanakarin J Sci Technol 29(2):529–541

Seshadri S, Saranya K, Kowshik M (2011) Green synthesis of lead sulfide nanoparticles by the lead resistant marine yeast, *Rhodosporidium diobovatum*. Biotechnol Prog 27(5):1464–1469. https://doi.org/10.1002/btpr.651

Shah S, Ghosh S (2020) Medicinal prospects of marine flora and fauna for drug discovery. In: Nathani NM, Mootapally CS, Gadhvi IR, Maitreya B, Joshi CG (eds) Marine niche: applications in pharmaceutical sciences—translational research. Springer Nature, Singapore, pp 321–345. Online ISBN: 978–981–15-5017-1; Print ISBN: 978-981-15-5016-4. https://doi.org/10.1007/978-981-15-5017-1_18

Sharma N, Pinnaka AK, Raje M, Fnu A, Bhattacharyya MS, Choudhury AR (2012) Exploitation of marine bacteria for production of gold nanoparticles. Microb Cell Fact 11:86. https://doi.org/10.1186/1475-2859-11-86

Shende S, Joshi KA, Kulkarni AS, Shinde VS, Parihar VS, Kitture R, Banerjee K, Kamble N, Bellare J, Ghosh S (2017) *Litchi chinensis* peel: a novel source for synthesis of gold and silver nanocatalysts. Glob J Nanomed 3(1):555603

Shende S, Joshi KA, Kulkarni AS, Charolkar C, Shinde VS, Parihar VS, Kitture R, Banerjee K, Kamble N, Bellare J, Ghosh S (2018) *Platanus orientalis* leaf mediated rapid synthesis of catalytic gold and silver nanoparticles. J Nanomed Nanotechnol 9(2):494. https://doi.org/10.4172/2157-7439.1000494

Shinde SS, Joshi KA, Patil S, Singh S, Kitture R, Bellare J, Ghosh S (2018) Green synthesis of silver nanoparticles using *Gnidia glauca* and computational evaluation of synergistic potential with antimicrobial drugs. World J Pharm Res 7(4):156–171

Shunmugam R, Balusamy SR, Kumar V, Menon S, Lakshmi T, Perumalsamy H (2021) Biosynthesis of gold nanoparticles using marine microbe (*Vibrio alginolyticus*) and its anticancer and antioxidant analysis. J King Saud Univ Sci 33(1):101260. https://doi.org/10.1016/j.jksus.2020.101260

Tawre MS, Shiledar A, Satpute SK, Ahire K, Ghosh S, Pardesi K (2022) Synergistic and antibiofilm potential of *Curcuma aromatica* derived silver nanoparticles in combination with antibiotics against multi drug resistant pathogens. Front Chem 10:1029056. https://doi.org/10.3389/fchem.2022.1029056

Vala AK (2015) Exploration on green synthesis of gold nanoparticles by a marine-derived fungus Aspergillus sydowii. Environ Prog Sustain Energy 34(1):194–197. https://doi.org/10.1002/ep.11949

Valarmathi N, Ameen F, Almansob A, Kumar P, Arunprakash S, Govarthanan M (2020) Utilization of marine seaweed *Spyridia filamentosa* for silver nanoparticles synthesis and its clinical applications. Mater Lett 263:127244. https://doi.org/10.1016/j.matlet.2019.127244

Zhang C, Kim SK (2010) Research and application of marine microbial enzymes: status and prospects. Mar Drugs 8(6):1920–1934. https://doi.org/10.3390/md8061920

Zhang L, An R, Wang J, Sun N, Zhang S, Hu J, Kuai J (2005) Exploring novel bioactive compounds from marine microbes. Curr Opin Microbiol 8(3):276–281. https://doi.org/10.1016/j.mib.2005.04.008

Zhou H, Pan H, Xu J, Xu W, Liu L (2016) Acclimation of a marine microbial consortium for efficient Mn (II) oxidation and manganese containing particle production. J Hazard Mater 304:434–440. https://doi.org/10.1016/j.jhazmat.2015.11.019